



ELSEVIER

Earth and Planetary Science Letters 126 (1994) 275–287

EPSL

The North Atlantic atmosphere–sea surface ^{14}C gradient during the Younger Dryas climatic event

Edouard Bard ^a, Maurice Arnold ^b, Jan Mangerud ^c, Martine Paterne ^b,
Laurent Labeyrie ^b, Josette Duprat ^d, Marie-Antoinette Mélières ^e,
Eivind Sønstegaard ^f, Jean-Claude Duplessy ^b

^a CEREGE, CNRS–Université d'Aix-Marseille III, JE 192, sce 431, Faculté de St Jérôme, 13397 Marseille Cedex 20, France

^b Centre des Faibles Radioactivités, CNRS–CEA, F-91198 Gif-sur-Yvette Cedex, France

^c Department of Geology, University of Bergen, Allégt. 41, N-5007 Bergen, Norway

^d Département de Géologie et Océanographie, Université de Bordeaux I, Bordeaux I, France

^e Laboratoire de Glaciologie et Géophysique de l'Environnement, BP96, 38402 St Martin d'Hères, France

^f Sogn og Fjordane College, N-5801 Sogndal, Norway

Received 29 March 1994; revision accepted 14 July 1994

Abstract

We attempt to quantify the ^{14}C difference between the atmosphere and the North Atlantic surface during a prominent climatic period of the last deglaciation, the Younger Dryas event (YD). Our working hypothesis is that the North Atlantic may have experienced a measurable change in ^{14}C reservoir age due to large changes of the polar front position and variations in the mode and rate of North Atlantic Deep Water (NADW) production.

We dated contemporaneous samples of terrestrial plant remains and sea surface carbonates in order to evaluate the past atmosphere–sea surface ^{14}C gradient. We selected terrestrial vegetal macrofossils and planktonic foraminifera (*Neogloboquadrina pachyderma* left coiling) mixed with the same volcanic tephra (the Vedde Ash Bed) which occurred during the YD and which can be recognized in North European lake sediments and North Atlantic deep-sea sediments. Based on AMS ages from two Norwegian sites, we obtained about 10,300 yr BP for the 'atmospheric' ^{14}C age of the volcanic eruption. Foraminifera from four North Atlantic deep-sea cores selected for their high sedimentation rates ($> 10 \text{ cm kyr}^{-1}$) were dated by AMS (21 samples). For each core the raw ^{14}C ages assigned to the ash layer peak is significantly older than the ^{14}C age obtained on land. Part of this discrepancy is due to bioturbation, which is shown by numerical modelling. Nevertheless, after correction of a bioturbation bias, the mean ^{14}C age obtained on the planktonic foraminifera is still about 11,000–11,100 yr BP. The atmosphere–sea surface ^{14}C difference was roughly 700–800 yr during the YD, whereas today it is 400–500 yr. A reduced advection of surface waters to the North Atlantic and the presence of sea ice are identified as potential causes of the high ^{14}C reservoir age during the YD.

1. Introduction

Numerous studies have demonstrated that the mode, rate and location of North Atlantic Deep

Water (NADW) production were quite variable during the Quaternary and, in particular, during two recent cold periods, the last glacial maximum (LGM, about 18 kyr BP [1–5]) and the Younger

Dryas event (YD, about 11–10 ^{14}C kyr BP, [6–10]). Nevertheless, despite the number of investigations and the variety of paleoceanographic proxies (benthic microfauna, $\delta^{13}\text{C}$, $\delta^{18}\text{O}$, Cd/Ca, Ba/Ca), no unique reconstruction of the glacial-like North Atlantic circulation has emerged. Moreover, the individual tracers used in earlier studies are sometimes in conflict with each other, for reasons which are poorly understood.

In addition, calibration of ^{14}C ages has demonstrated that the atmospheric $^{14}\text{C}/^{12}\text{C}$ ratio varied widely during the last 20 kyr, and in particular that very abrupt $^{14}\text{C}/^{12}\text{C}$ changes occurred during the last deglaciation (creating the so-called ^{14}C age plateaus [11]). Although the long-term atmospheric $^{14}\text{C}/^{12}\text{C}$ ratio decrease is attributed to cosmic ray production changes [12,13], the rapid variations are probably linked to changes in the ^{14}C distribution between the different carbon reservoirs. In a recent study, changes in NADW production were invoked to explain the major $^{14}\text{C}/^{12}\text{C}$ decrease of about 100‰ which occurred at the end of the YD [14].

In this paper we attempt to complement the picture with an independent tracer, the atmosphere–sea surface ^{14}C gradient (also expressed as the sea surface ^{14}C reservoir age). For the present-day ocean the sea surface ^{14}C reservoir age is of the order of 300–400 yr at low latitudes and rises to 1200 yr at higher latitudes in the Southern Ocean and the North Pacific (Fig. 1). High-latitude surface waters are old because of upwelling of subsurface water, whose $^{14}\text{C}/^{12}\text{C}$ is not reset to atmospheric values.

By contrast, no surface ^{14}C gradient is present between 40° and 70°N in the North Atlantic Ocean (Fig. 1). The apparent natural ^{14}C age of these surface waters is almost constant, at about 400–500 yr. This is linked to the northward advection of surface and thermocline waters from lower latitudes which travel through the Gulf Stream and North Atlantic current systems. After recirculation and winter convection, this water flux ultimately feeds the NADW.

The ^{14}C reservoir age should be sensitive to changes in the mode, rate and location of NADW production. As a first use of this approach, we attempted to evaluate the past atmosphere–sea

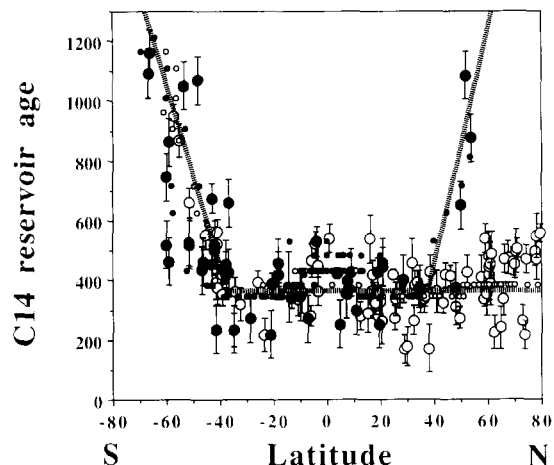


Fig. 1. Pre-anthropogenic distribution of the ^{14}C reservoir age in the Atlantic (\circ) and in the Pacific and Indian Oceans (\bullet). Most data correspond to seawater samples collected before 1957, which partly explains the spread and the large errors of these early ^{14}C measurements. A small correction for the injection of fossil fuel has been applied (see [26] for details). The smaller symbols correspond to data obtained during the GEOSECS (1972) and TTO (1981) expeditions. Those data have also been corrected for the bomb-produced ^{14}C by using the tritium– ^{14}C correlation [48].

surface ^{14}C gradient during the YD. Contemporaneous samples of terrestrial organic matter and sea surface carbonates were dated by AMS and the ^{14}C age difference was used to quantify the past reservoir age. In order to ensure strict contemporaneity of the samples, we selected terrestrial vegetal macrofossils and planktonic foraminifera mixed with the same instantaneous time marker, a volcanic ash layer from Iceland which was deposited during the YD and which can be characterized through chemical analyses and firmly correlated between North European lake sediments and North Atlantic deep-sea sediments [15,16]. This ash is named the Vedde Ash Bed, or, in the North Atlantic, Ash Zone I. The Vedde Ash is found approximately in the middle of the YD, as identified both with lithostratigraphy and pollen in continental sediments and with $\delta^{18}\text{O}$ and the foraminifera distribution in oceanic sediments. On the continent the volcanic ash is windblown [15], whereas in the deep-sea sediments the ash shards were also rafted by drifting sea ice [17]. Nevertheless, the delay in deposition

was only a few years or at a maximum a few decades [16] and the rhyolitic tephra can be used as a geologically instantaneous time marker.

2. Land data

Vegetal macrofossils bracketing the Vedde Ash were dated by AMS at two Norwegian sites (Fig. 2), the type section Torvlømyra [15] and the paleolake Heggjadalsetra [Sønstegaard, in prep.]. The samples from Torvlømyra were sieved at $125\ \mu\text{m}$ and the terrestrial plant remains were selected by Dr. H. Birks of the Botany Department of the University of Bergen. The samples from Heggjadalsetra are different species of mosses found within the Ash Bed in two cores. The AMS results are listed on Table 1 and the results from

Torvlømyra are also reported on the stratigraphic log shown in Fig. 3. For this site the pollen stratigraphy and a complete sedimentological description can be found in [18].

In the case of Torvlømyra, we were obliged to measure ^{14}C ages in very small samples (typically less than 0.5 mg of carbon), which would explain the high statistical errors obtained for ages from this site. In addition, special experiments were conducted on vegetal fossils to quantify the chemistry blanks associated with such small samples (i.e., slight contamination during the target preparation). Specifically, we measured ^{14}C ages of small pieces of plant collected in the Eemien section of the Grande Pile peat bog with sizes ranging between 0.1 and 2 mg of carbon (Table 2). The results demonstrate that the ^{14}C chemistry blank is rather low for samples as small as

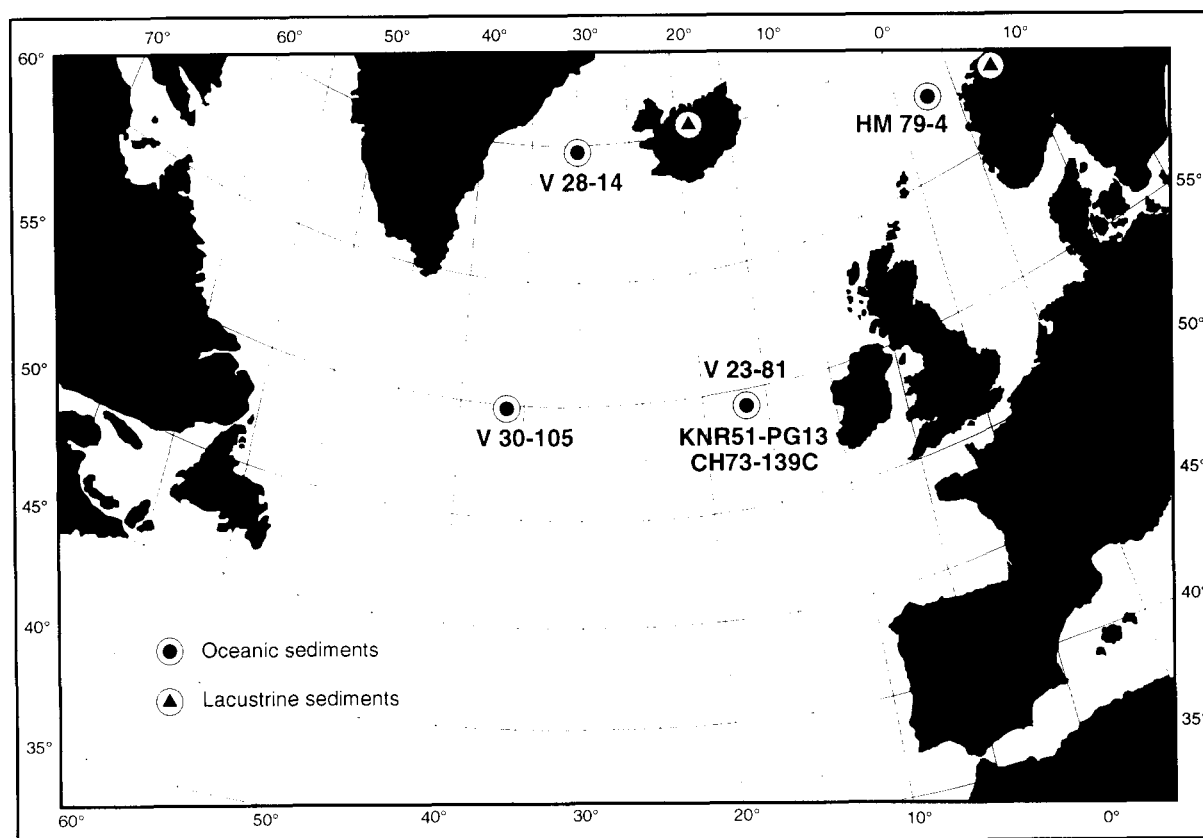


Fig. 2. Locations of sediment cores studied or cited in the discussion.

0.1 mgC. These blanks were subtracted to calculate the ^{14}C ages for the Torvlømyra macrofossils.

Based on five AMS ages from the two Norwegian sites, we calculate a mean ^{14}C age of about 10,300 yr BP for the volcanic eruption. This is close to the ^{14}C ages previously published for

Norwegian paleolakes ([15], classical β -counting on large samples) and for Lake Torfadalsvatn in Iceland ([19], by AMS on selected samples). The dated samples consisted of terrestrial plants, which should eliminate the problem of the hard water effect (incorporation of old bicarbonate

Table 1

AMS ^{14}C results obtained on the Vedde Ash Layer from land and marine sediments. The land data were obtained on terrestrial vegetal material and the marine data on picked samples of *Neogloboquadrina pachyderma* left coiling. All ages are raw conventional ^{14}C ages expressed in yr BP. Reworking or the presence of burrows could explain the difference from an isolated ^{14}C age of $11,100 \pm 100$ yr BP at 128 cm in core KN51-PG13 [21] (see text).

Sample identification	mg of C	^{14}C age (yr BP)	1 σ error	AMS Lab. n°.
Land Data				
Heggyadalsetra 1	>1	10325	115	TUa-298
Heggyadalsetra 2	>1	10360	80	TUa-299
Torvlømyra 640-642cm	0.17	10430	240	GifA-91244
Torvlømyra 628-638cm	0.19	9050	280	GifA-91245
Torvlømyra 623-626cm	0.13	10040	260	GifA-92307
Torvlømyra 623-626cm	0.34	9950	160	GifA-91235
Marine Data				
V23-81 172-173cm	0.8	11980	110	ETH-4656
V23-81 160-161cm	1.5	11380	150	GifA-90183
V23-81 157-158cm	1.0	11470	140	GifA-90184
V23-81 157-158cm	0.9	11280	90	ETH-4193
V23-81 154-155cm	2.1	10800	170	GifA-90185
V23-81 150-151cm	1.6	11110	140	GifA-90186
V23-81 141-143cm	0.5	10940	150	GifA-90191
V28-14 115-117cm	1.9	12010	160	GifA-90197
V28-14 107-109cm	1.2	11440	130	GifA-90198
V28-14 102-104cm	1.3	11280	130	GifA-90199
V28-14 94-96cm	1.0	10690	130	GifA-91071
V28-14 90-91cm	1.7	9210	140	GifA-89073
V30-105 106-107cm	1.6	13370	130	GifA-91016a,b
V30-105 97-98cm	1.5	12020	110	GifA-91015a,b
V30-105 90-91cm	1.7	11110	100	GifA-91014a,b
V30-105 87-88cm	1.4	11680	110	GifA-91018a,b
V30-105 81-82cm	1.0	11780	150	GifA-91070
V30-105 73-74cm	1.2	11360	100	GifA-91017
KN51 PG13 132-133cm	1.2	11720	150	GifA-90194
KN51 PG13 129-130cm	1.4	11950	140	GifA-90196
KN51 PG13 127-128cm	1.3	12150	160	GifA-90193
KN51 PG13 123-124cm	1.6	11980	130	GifA-90192

AMS laboratories: GifA = CFR Gif-sur-Yvette; TUa = preparation in Trondheim, AMS in Uppsala; ETH = Zürich (from [46]). The foraminifera sample in V23-81 at 157–158 cm was homogenized and split in two halves which were measured separately by AMS at Gif-sur-Yvette (GifA-90184) and the ETH (ETH-4193, [46]). The iron-carbon mixtures synthesized for the first four samples of core V30-105 were split in two halves and measured separately by AMS (runs 'a' and 'b'). The weighted mean age of the two individual results is given.

Table 2

Blank samples obtained on small pieces of plant from the Eemien (~ 125,000 yr BP) section of the Grande Pile peat bog

Sample	mg of C	¹⁴ C % modern C	1 σ error	¹⁴ C age yr BP	$\pm 1\sigma$
GP7	1.68	0.23	0.03	48800	1200
GP9	1.44	0.18	0.03	50900	1300
GP8	1.19	0.27	0.03	47500	960
GP5	0.33	0.74	0.08	39430	880
GP1	0.30	0.62	0.06	40780	800
GP4	0.28	0.80	0.12	38800	1200
GP6	0.24	0.53	0.07	42100	1000
GP3	0.17	0.73	0.10	39500	1100
GP2	0.15	0.76	0.14	39200	1500

Measurements performed on the Tandetron at Gif-sur-Yvette

dissolved in the lake). In the following discussion we will refer to this mean age (10,300 yr BP) as the 'atmospheric' age of the ash layer.

3. Marine data

We studied four deep-sea cores from the North Atlantic (55–65°N) that were selected for their high sedimentation rates (> 10 cm kyr⁻¹). These are core V23-81, V28-14, V30-105 and KNR51-PG13 (Table 3). Counts of rhyolitic ash shards for the four cores [20,21] and microprobe analytical results [15,16] for cores V28-14 and V23-81 were published previously. The new chemical analyses of the glass shards presented here were obtained by means of a scanning electron microscope coupled to an X-ray energy dispersion spectrometer. Our measurements (Table 4) confirm the results previously obtained on the glass chemistry both from the cores mentioned and from other cores of lacustrine and deep-sea sediments [15,16]. Most

glass shards from Ash Zone 1 have a rhyolitic composition. A diagnostic feature of the Vedde Ash is the high Fe content compared to other Icelandic rhyolitic ashes.

The stratigraphic position of the rhyolitic ash layer was checked further by measuring the $\delta^{18}\text{O}$ composition of hand-picked foraminifera mixed with the rhyolitic ash shards (*Neogloboquadrina pachyderma* left coiling). The isotopic results (Table 5) are in excellent agreement with YD $\delta^{18}\text{O}$ values from records of the last deglaciation previously published for cores V23-81 ([22], Fig. 4), V28-14 ([23], Fig. 4) and CH73-139C [24].

The *N. pachyderma* left coiling samples aliquoted for $\delta^{18}\text{O}$ analysis were also dated by AMS (Table 1 and Fig. 5, ages are raw conventional ¹⁴C ages in yr BP). A ¹⁴C age for the ash layer peak was estimated by using a linear regression through the ¹⁴C data. This peak age is of the order of 11,300, 11,600, 11,900 and 11,900 ¹⁴C yr BP for cores V23-81, V28-14, V30-105 and KNR51-PG13 respectively, the mean being close

Table 3

Location of deep-sea cores discussed in the text

Core	Latitude	Longitude	Water depth (m)
V23-81	54°15'N	16°50'W	2393
V28-14	64°47'N	29°34'W	1855
V30-105	54°31'N	36°30'W	2758
KN51-PG13	54°28'N	15°18'W	2665
HM79-4	63°06'N	02°33'E	983
CH73-139C	54°38'N	16°21'W	2209

to 11,700 yr. This average is in agreement with an individual ^{14}C AMS age ($11,625 \pm 180$ ^{14}C yr BP) obtained on the ash layer from core HM79-4 [25].

4. Bioturbation bias

Taken at face value these oceanic ages are much older than the mean age of the ash layer obtained on continental sediments (10,300 ^{14}C yr BP). However, part of this difference may be due to bioturbation, which mixes downward ash layers and foraminifera in deep-sea sediments. Consequently, we performed a numerical simulation in order to simulate the bias created by bioturbation (see [24] for details of the numerical procedure). Two different impulse response functions were used to simulate intense mixing and weak mixing. These two extreme cases resulted in different shapes for the bioturbated ash layer: an exponential decay for intense bioturbation, and a symmetrical triangle-like distribution for weak mixing. In the case of weak mixing no significant bias is created between the ash layer peak and the foraminiferal age. In the case of intense mixing the age bias varies between zero and a few centuries depending on the mixing depth and the average sedimentation rate of the core. Figs. 6a and b show an example of such a simulation,

whereas Fig. 6c represents the age bias calculated for bioturbation depths ranging between 0 and 14 cm and typical sedimentation rates (8, 12 and 17 cm kyr^{-1}). More details on the simulations will be published elsewhere.

For cores V23-81, V30-105 and V28-14 we estimated apparent mixing depths by least-square fitting exponential curves on the tails of the glass shards distributions (cf. Figs. 5a–c). Then, first order corrections were determined to correct the raw ^{14}C ages of the ash layer peaks: 300, 600 and 550 yr for cores V23-81, V28-14 and V30-105 respectively. For core KNR51-PG13 the ash layer is irregular and cannot be fitted by an exponential curve. The low abundance and the spread of the rhyolitic glass shards suggest that the bioturbation was intense and irregular for this particular core section (reworking or presence of burrows?), and we set arbitrarily an upper bound for its equivalent bioturbation depth (i.e., 20 cm).

It was then possible to calculate a corrected ash layer age for each core: 11,000, 11,000, 11,300 and $\sim 11,100$ ^{14}C yr BP for cores V23-81, V28-14, V30-105 and KNR51-PG13 respectively. The mean ^{14}C age assigned to the rhyolitic eruption is thus of the order of 11,000–11,100 ^{14}C yr BP, which is still significantly older than the ^{14}C age obtained on land (about 10,300 ^{14}C yr BP).

Table 4

Summary of microprobe measurements performed on rhyolitic glass shards in the samples used for AMS dating

Sample (core,depth)	Number of glass shards	Na ₂ O %	Al ₂ O ₃ %	SiO ₂ %	K ₂ O %	CaO %	FeO _{tot} %
V23-81, 150-151	37	5.48 (0.36)	13.28 (0.21)	71.07 (0.47)	3.56 (0.14)	1.31 (0.09)	4.03 (0.33)
V23-81, 154-155	36	5.43 (0.37)	13.27 (0.23)	71.14 (0.34)	3.57 (0.12)	1.31 (0.10)	3.98 (0.25)
V23-81, 160-161	38	5.50 (0.32)	13.16 (0.24)	71.26 (0.43)	3.61 (0.14)	1.30 (0.13)	3.96 (0.17)
V28-14, 94-96	33	5.38 (0.39)	13.24 (0.19)	71.28 (0.45)	3.57 (0.14)	1.33 (0.11)	4.05 (0.27)
V28-14, 102-104	27	5.34 (0.30)	13.19 (0.19)	71.39 (0.36)	3.62 (0.08)	1.34 (0.09)	4.02 (0.21)
V28-14, 107-109	27	5.37 (0.32)	13.28 (0.21)	71.33 (0.44)	3.59 (0.14)	1.31 (0.12)	4.02 (0.24)
V30-105, 80-82	31	5.29 (0.40)	13.41 (0.18)	71.33 (0.44)	3.59 (0.14)	1.30 (0.12)	3.91 (0.23)
V30-105, 89-90	23	5.31 (0.38)	13.36 (0.19)	71.26 (0.50)	3.59 (0.15)	1.30 (0.10)	3.93 (0.23)
KN51-PG13, 114-115	40	5.42 (0.32)	13.19 (0.31)	71.16 (0.68)	3.55 (0.20)	1.37 (0.26)	4.08 (0.38)
KN51-PG13, 129-130	33	5.41 (0.37)	13.12 (0.23)	71.46 (0.52)	3.61 (0.14)	1.29 (0.12)	3.99 (0.30)

Measurements performed by means of the SEM–EDS system in Gif-sur-Yvette. Standard deviations calculated from the spread of the individual measurements obtained on each depth (27 to 40 shards) are given in parentheses.

5. Interpretation of the data

The 700–800 yr difference between the ‘atmospheric’ age and the ‘sea surface’ age of the rhyolitic eruption compared with the present value of about 400–500 yr may thus be interpreted as due to a small but genuine increase in the North Atlantic sea surface $\Delta^{14}\text{C}$.

In principle, a steady-state change in the sea surface $\Delta^{14}\text{C}$ could be a response to a variety of phenomena, such as changes in atmospheric CO_2 concentration, sea surface temperature (SST), ice cover, wind speed and deep-sea ventilation (see [26] for first-order modelling).

From direct gas measurements along Antarctica and Greenland ice cores we know that the

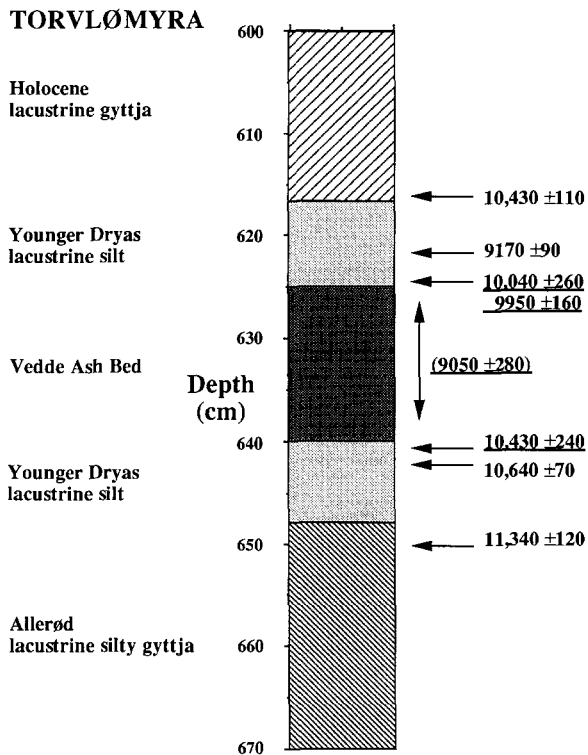


Fig. 3. Simplified stratigraphic log for Torvlømyra. Underlined ages have been obtained by AMS on vegetal macrofossils. The other ages were obtained on bulk sediment by β -counting [15]. The age of 9050 ± 280 ^{14}C yr BP is undoubtedly a flier: in contrast to the other samples, which were obtained in a 3 cm depth interval, this particular sample was obtained by gathering the rare macrofossils spread in the ash layer. This could explain a much higher contamination by recent carbon.

Table 5

$\delta^{18}\text{O}$ obtained on subsamples of the *N. pachyderma* left coiling samples used for AMS

Sample	$\delta^{18}\text{O}$ (‰ vs PDB)
V23-81 160-161cm	2.98
V23-81 154-155cm	2.84
V23-81 150-151cm	2.82
V23-81 141-143cm	2.91
V28-14 115-117cm	3.42
V28-14 115-117cm	3.57
V28-14 107-109cm	2.95
V28-14 102-104cm	3.11
V28-14 94-96cm	2.88
V28-14 94-96cm	2.94
V30-105 106-107cm	3.31
V30-105 97-98cm	3.36
V30-105 90-91cm	3.17
V30-105 87-88cm	3.52
V30-105 81-82cm	2.81
V30-105 73-74cm	3.36
KN51 PG13 132-133cm	2.61
KN51 PG13 129-130cm	2.91
KN51 PG13 127-128cm	3.07
KN51 PG13 123-124cm	3.24
KN51 PG13 123-124cm	3.05
KN51 PG13 114-115cm	2.88

Measurements performed on a MAT-Finnigan 251 mass spectrometer in Gif-sur-Yvette.

CO_2 concentrations were of the order of 230 and 280 ppmv for the YD and pre-industrial periods respectively [27]. Consequently, the sea surface $\Delta^{14}\text{C}$ was probably lower by about 11‰, corresponding to an increase in the reservoir age of about 90 yr.

A decrease in temperature affects the solubility of CO_2 (increases), the piston velocity (decreases) and the kinetic isotopic fractionation factors (increases). However, the overall effect is rather small since the different components vary in opposite directions [28]. Foraminifera and diatom species distribution can be used to quantify the North Atlantic SSTs during the YD. In Table 6 we listed the SSTs estimated on the samples used for AMS by using the best analogue method. These data indicate that the sea surface was indeed much colder than today during the YD, in accordance with previous studies [29,30]. However, an accurate quantification of the cooling is

still difficult, for two main reasons: bioturbation tends to decrease the amplitude of the YD cooling, and the foraminifera transfer functions are not very precise below 7°C in winter and 10°C in summer. In order to illustrate bioturbation smoothing, we can cite the example of the YD level in core CH73-139C characterized by a sedimentation rate of about 10 cm kyr⁻¹. For the YD level, winter and summer SSTs estimated by using deconvolved foraminiferal abundances are about 2°C lower than those obtained with the raw counts ([30] and new calculations using the best analogue method). Based on a diatom transfer function, winter and summer SSTs of the order of -2°C and 2°C were estimated for the YD section in core HM79-4 [25]. Altogether, the transfer function data suggest that a maximum cooling of about 10°C occurred during the YD. The net effect is a decrease in the reservoir age by a few decades, which can be ignored in the present study.

During the YD and LGM periods, the northern polar front was roughly zonal at about 40°N, and for sites located north of 50°N, sea ice cover was present through part of the year [20]. This was confirmed by the study of diatom assemblages, which indicate an important sea ice cover during the YD [25,31]. The presence of sea ice severely limits the ocean-atmosphere gas exchange and thus increases the sea surface ¹⁴C reservoir age (see [32] for a recent study of the modern distribution of ¹⁴C in the Weddell Sea). A box model which simulates the carbon cycle (Fig. 7) was used to quantify the effect on the North Atlantic surface. The results obtained for the North Atlantic surface box for sea ice cover varying between 0 and 12 month/yr leads to ¹⁴C reservoir age increases up to 350 yr (Fig. 8). To a first approximation, we shall assume that for sites located north of 50°N sea ice was present for at least half the year during the YD. This may explain an increase in reservoir age of at least 120 yr (Fig. 8).

Reconstruction of the chemistry of Greenland ice cores indicates that the flux of marine aerosols (Cl⁻, Na⁺, K⁺) was increased by 50–100% during the YD [33]. An increased wind strength alone cannot account for the chemical flux distri-

bution and the complete set of aerosol data requires changes in sources and transport paths [33]. Nevertheless, as an upper bound we shall assume that the marine aerosol increase in the YD was mainly due to a change in wind speed. By means of empirical formulae [34,35] it is then possible to estimate an upper bound of about 50% for the wind speed increase during the YD. Such a wind speed increase applied to the North Atlantic surface would undoubtedly lead to an increase in the CO₂ piston velocity [36] and consequently to a decrease in the ¹⁴C reservoir age. By

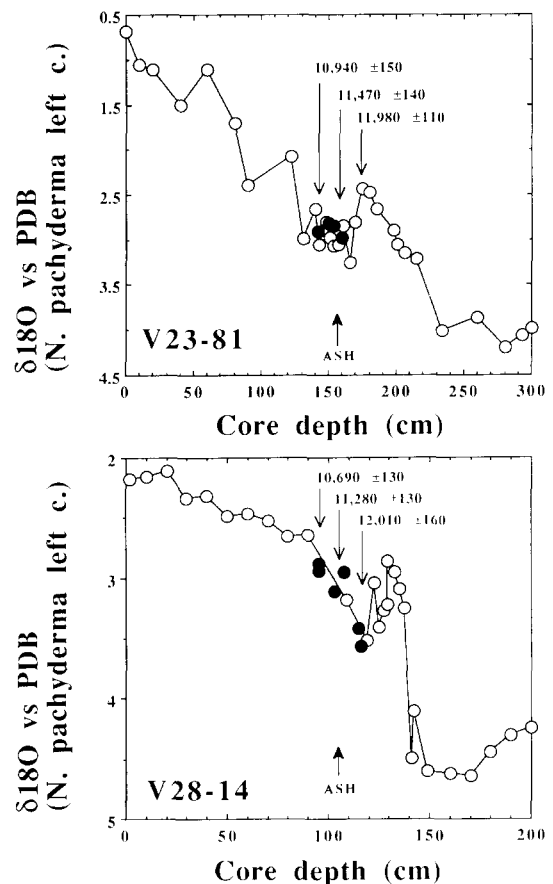


Fig. 4. $\delta^{18}\text{O}$ records for cores V23-81 and V28-14. \circ = Data published previously ([22] and [23] for cores V23-81 and V28-14 respectively). \bullet = $\delta^{18}\text{O}$ data (Table 5) measured on *N. pachyderma* left coiling aliquoted from the same samples used for AMS analyses. Only a few AMS ¹⁴C ages are indicated (see Table 1 for the complete data list).

using the box model we calculate about 130 yr as an upper bound for this decrease (Figure 8).

A transient change of sea surface $\Delta^{14}\text{C}$ could also be due to a rapid shift in the atmospheric $^{14}\text{C}/^{12}\text{C}$ ratio linked to a variation in the ^{14}C production. Indeed, it has been shown [37,12–14] that the end of the YD was a period characterized by a drastic decrease in the atmospheric $^{14}\text{C}/^{12}\text{C}$ ratio. At steady state, the sea surface $\Delta^{14}\text{C}$ is left unchanged by production variations.

However, since the oceanic $^{14}\text{C}/^{12}\text{C}$ adjustment lags behind its atmospheric counterpart, a transient decrease in the sea surface ^{14}C reservoir age may have accompanied the rapid fall in the atmospheric $^{14}\text{C}/^{12}\text{C}$ ratio. By assuming an instantaneous production drop of 10%, the model produces a small transient reduction in the ^{14}C reservoir age of about 30 yr.

So far the different variations are rather small, each being less than 350 yr in absolute terms.

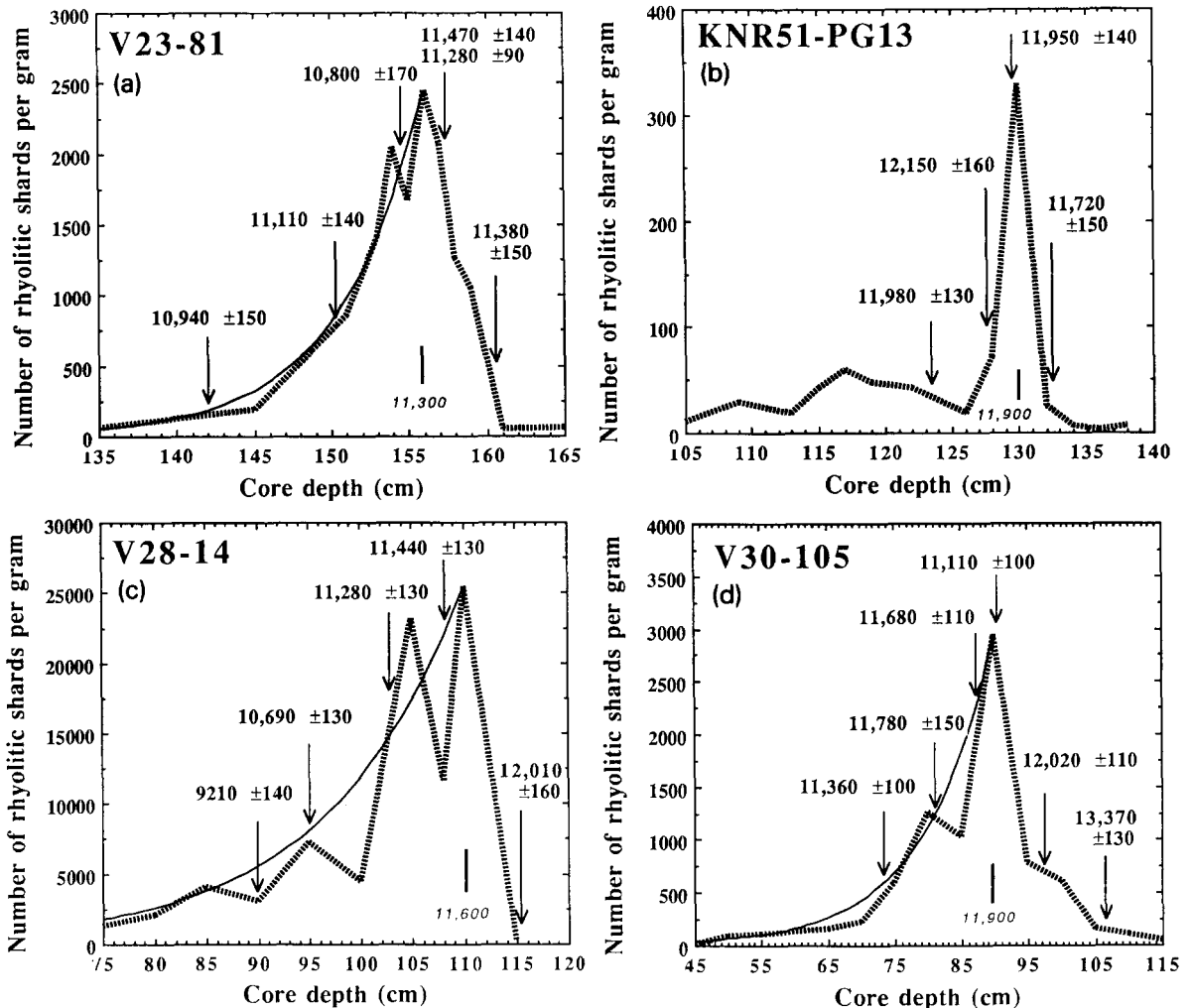


Fig. 5. Rhyolitic glass shard distribution and ^{14}C ages obtained on four deep-sea cores (note that the ^{14}C ages are not corrected for reservoir age). The glass-shard counts can be found in [20] (shards > 63 μm) and [21] (shards > 150 μm , for KNR51-PG13 only). Exponential fits of the distribution tails for cores V23-81, V28-14 and V30-105 are also represented (see text). They were used to calculate upper bounds on the bioturbation depths for each core (5, 13 and 10 cm for V23-81, V28-14 and V30-105 respectively). Under the curves are given the mean raw ^{14}C ages of the ash peaks.

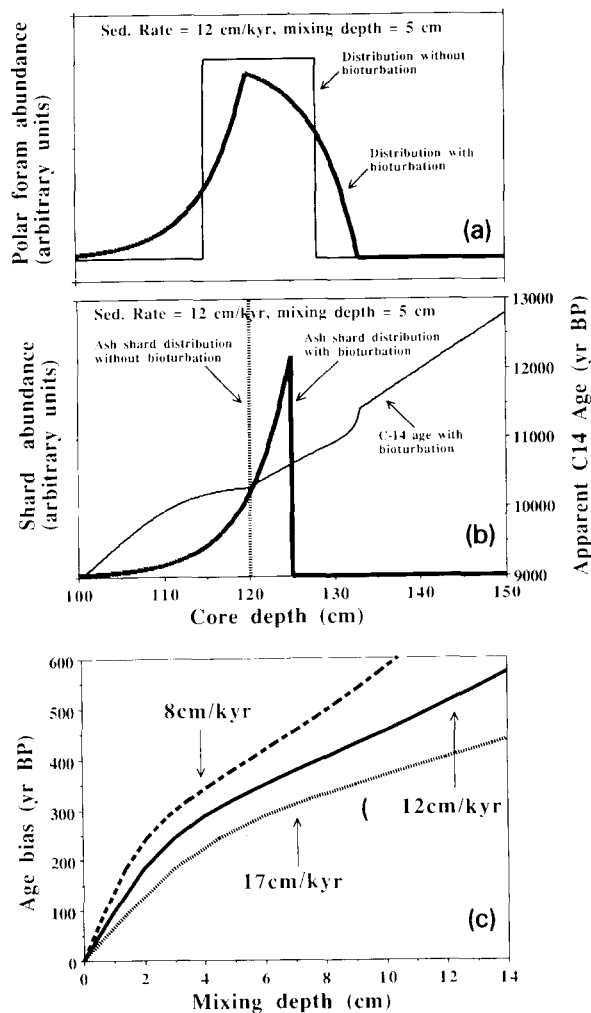


Fig. 6. Simulation of the age bias due to bioturbation. Figs. 6a and b correspond to one particular simulation with a sedimentation rate of 12 cm kyr⁻¹ and a mixing depth of 5 cm. Fig. 6a presents the abundance of polar foraminifera (*N. pachyderma* left coiling) with and without bioturbation. In this particular example the polar foraminiferal abundance is increased by a factor of 10 during the YD [24]. The simulations are performed in calendar years and then converted into ¹⁴C ages. This problem is of secondary importance since the ¹⁴C calibration curve is almost linear between the two ¹⁴C age plateaus at 12,600 and 10,000 ¹⁴C yr BP [13,14]. Fig. 6b presents the bioturbated shard distribution and the relationship between ¹⁴C age and depth after bioturbation. Fig. 6c summarizes numerous simulations of that type obtained for three different sedimentation rates and mixing depth. The age bias is the difference between the true age of the eruption and the apparent ¹⁴C age of the ash peak. A complete description will be presented elsewhere to give more details on the individual simulations used for obtaining this summary plot.

Moreover, the combination of the different contributions would tend to cancel out and the net effect of all the estimates listed above should not exceed 300 yr. The change in ¹⁴C reservoir age observed during the YD may also be a response to a variation in the Atlantic circulation. In his hypothetical reversal of the Glacial Atlantic, Broecker [38] calculated a ¹⁴C reservoir age of about 900 yr. Such a mode of circulation is similar to Southern Sinking states observed in oceanic general circulation models [39,40]. If real, this mode would alone explain the sea surface ¹⁴C data reconstructed in the present study. However, numerous proxy data records have now been generated showing that the Atlantic circulation change during the YD was not as dramatic as a full reversal. These reconstructions are based on faunal [8,9], chemical (Cd/Ca [6]) and isotopic

Table 6

Transfer function SST estimates obtained on samples used for AMS. The best analogue method has been used for each level (ten modern analogues). In bold are the mean modern SSTs calculated for the core sites by using the *Levitus Atlas* database [47]. The coldest level in core V23-81 is at 157 cm, with an estimated SST of 2°C [29], or 3.2 ± 2.7°C by using the modern analogue technique.

Sample	February SST °C (±1sigma)	August SST °C (±1sigma)
Today	10.4	14.5
V23-81 160-161cm	5.5 (1.1)	10.2 (1.0)
V23-81 154-155cm	3.3 (1.0)	8.3 (1.0)
V23-81 150-151cm	5.3 (1.1)	10.2 (0.9)
V23-81 142-143cm	9.3 (1.1)	13.1 (1.2)
V23-81 141-142cm	8.4 (1.5)	12.4 (1.5)
Today	5.8	8.8
V28-14 115-117cm	0.2 (1.0)	5.5 (1.5)
V28-14 107-109cm	0.1 (1.2)	5.3 (1.4)
V28-14 102-104cm	1.3 (1.8)	6.3 (2.0)
V28-14 94-95cm	5.7 (0.9)	10.3 (0.8)
Today	5.2	11.3
V30-105 106-107cm	3.4 (1.2)	8.4 (1.3)
V30-105 97-98cm	3.0 (1.4)	8.4 (1.3)
V30-105 90-91cm	3.4 (1.6)	8.6 (1.7)
V30-105 87-88cm	4.0 (0.9)	9.1 (1.3)
V30-105 81-82cm	5.5 (1.2)	10.0 (0.9)
V30-105 73-74cm	7.2 (2.0)	10.9 (1.8)
Today	10.3	14.5
KN51 PG13 132-133cm	5.9 (1.0)	10.1 (1.0)
KN51 PG13 129-130cm	5.7 (1.1)	10.1 (1.0)
KN51 PG13 127-128cm	7.1 (1.5)	11.3 (1.4)
KN51 PG13 123-124cm	7.2 (1.5)	11.4 (1.4)

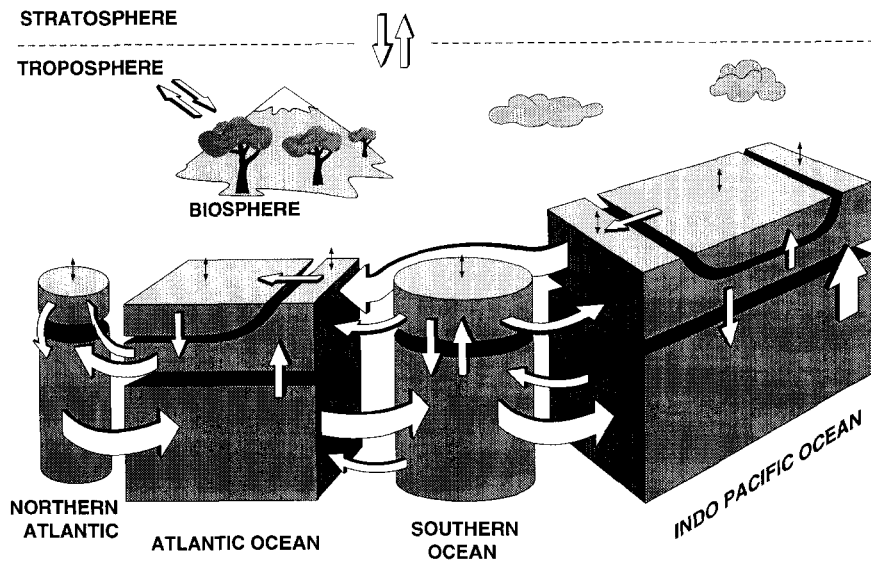


Fig. 7. Box model used to assess ^{14}C changes in the ocean (see text). This model is an hybrid of PANDORA [49] and the carbon cycle model in [50]. Details of the model will be published elsewhere.

($\delta^{13}\text{C}$ [8], $\delta^{18}\text{O}$ [10,22,42,43]) measurements determined on high sedimentation rate cores with sufficient time resolution. Most of them indicate that the NADW production never ceased completely during the YD, and instead was maintained ‘midway’ between the LGM and the modern circulation [42,43].

The ^{14}C increase observed in North Atlantic foraminifera does not necessarily require a cessation of the advection of nutrient-depleted waters to the North Atlantic. Indeed, physical oceanographers have shown that the circulation feeding the North Atlantic thermohaline convection is rather complex (see [44] for a recent review of the problem). About half of the source water transits the Gulf Stream and North Atlantic current system, being cooled on the way and finally sinking to form lower NADW, primarily in the Norwegian and Greenland Seas. The other half is a mixture of thermocline and upwelled intermediate waters which travels northward before sinking mainly in the Labrador Sea to form upper NADW. The near-surface half of the flow has a high-oxygen content, and hence a low ^{14}C age, being in immediate contact with the atmosphere, whereas the deeper half is depleted in oxygen and has a larger apparent ^{14}C age. Consequently, a partial reduction of the flow would affect differently the oceanic tracers: a shutdown of the near-surface component would affect the surface ^{14}C more than the nutrient distribution in the North Atlantic. This scenario is reasonable since during the LGM and YD the Gulf Stream ran zonally and the North Atlantic current system

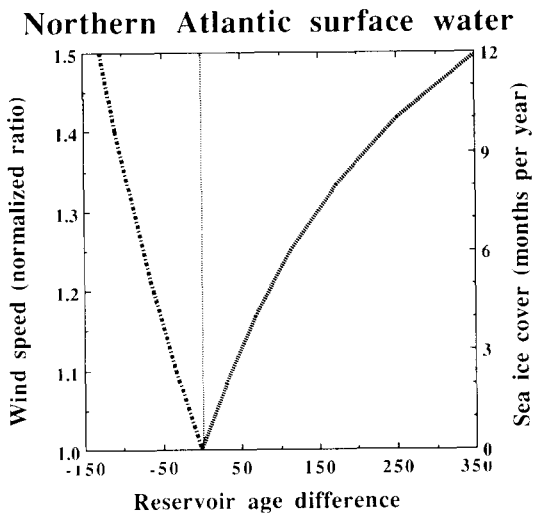


Fig. 8. ^{14}C age decrease in the Northern Atlantic surface box caused by wind speed increase (dashed lined) and ^{14}C age increase due to increased sea ice cover (dotted line).

was weak, if not absent [45]. The reduction of the near-surface flow would also explain the persistence of upper NADW and cessation of lower NADW production, which was replaced by Antarctic Bottom Water. This circulation scheme may thus be responsible for the temperature decrease and the ^{14}C reservoir age increase for the North Atlantic surface waters while maintaining sufficient transport of thermocline waters to feed a weaker NADW convection. A high ^{14}C reservoir age during the YD would thus be explained by a combination of two main phenomena: reduced advection of surface waters to the North Atlantic, and the presence of sea ice.

Acknowledgments

We thank H. Birks for selecting the terrestrial plant remains in the samples from Torvlømyra, R. Lotti for giving access to cores V28-14, V30-105 and V23-81 stored at the LDEO, L. Keigwin for giving access to core KNR51-PG13 stored at the WHOI, J.L. de Beaulieu for providing plant macrofossils from the Grande Pile peat bog, W.F. Ruddiman for providing published and unpublished data on shard counts in Ash Zone I, E. Boyle for fruitful discussion, and T. Johnson and J. Adams for correcting the manuscript. Support for this research was provided by the NSF (grant ATM 89-12377 to E. Bard), the CEA and the CNRS (PNEDC). [FA]

References

- [1] S.S. Streeter and N.J. Shackleton, Paleocirculation of the deep north Atlantic: 150,000-year record of benthic foraminifera and oxygen-18, *Science* 203, 168–171, 1979.
- [2] E.A. Boyle and L. Keigwin, Deep circulation of the North Atlantic over the last 200,000 years: geochemical evidence, *Science* 218, 784–787, 1982.
- [3] W.B. Curry and G.P. Lohmann, Reduced advection into the Atlantic Ocean deep eastern basins during the last glacial maximum, *Nature* 306, 577–580, 1983.
- [4] J.-C. Duplessy, N.J. Shackleton, R.G. Fairbanks, L. Labeyrie, D. Oppo and N. Kallel, Deep water source variations during the last climatic cycle and their impact on the global deep water circulation, *Paleoceanography* 3, 343–360, 1988.
- [5] D. Lea and E.A. Boyle, Foraminiferal reconstruction of barium distributions in water masses of the glacial oceans, *Paleoceanography* 5, 719–742, 1990.
- [6] E.A. Boyle and L. Keigwin, North Atlantic thermohaline circulation during the last 20,000 years linked to high-latitude surface temperature, *Nature* 330, 35–40, 1987.
- [7] W.S. Broecker, M. Andree, W. Wolfli, H. Oeschger, G. Bonani, J. Kennett and D. Peteet, The chronology of the last deglaciation: implications of the cause of the Younger Dryas event, *Paleoceanography* 3, 1–19, 1988.
- [8] L.D. Keigwin, G.A. Jones, S.J. Lehman and E.A. Boyle, Deglacial meltwater discharge, North Atlantic deep circulation, and abrupt climatic change, *J. Geophys. Res.* 96(9), 16811–16826, 1991.
- [9] S.J. Lehman and L.D. Keigwin, Sudden changes in North Atlantic circulation during the last deglaciation, *Nature* 356, 757–762, 1992a.
- [10] J.-C. Duplessy, L. Labeyrie, M. Arnold, M. Paterne, J. Duprat and T.C.E. van Weering, Changes in surface salinity of the north Atlantic Ocean during the last deglaciation, *Nature* 358, 485–488, 1993.
- [11] M. Stuiver, T.F. Brazunias, B. Becker and B. Kromer, Climatic, solar, oceanic and geomagnetic influences on Late Glacial and Holocene atmospheric $^{14}\text{C}/^{12}\text{C}$ change, *Quat. Res.* 35, 1–24, 1991.
- [12] E. Bard, B. Hamelin, R.G. Fairbanks and A. Zindler, Calibration of ^{14}C timescale over the past 30,000 years using mass spectrometric U-Th ages from Barbados corals, *Nature* 345, 405–410, 1990.
- [13] E. Bard, M. Arnold, R.G. Fairbanks and B. Hamelin, ^{230}Th , ^{234}U and ^{14}C ages obtained by mass spectrometry on corals, *Radiocarbon* 35, 191–199, 1993.
- [14] R.L. Edwards, J.W. Beck, G.S. Burr, D.J. Donahue, J.M.A. Chappell, A.L. Bloom, E.R.M. Druffel and F.W. Taylor, A large drop in atmospheric $^{14}\text{C}/^{12}\text{C}$ and reduced melting in the Younger Dryas documented with ^{230}Th ages of corals, *Science* 260, 962–968, 1993.
- [15] J. Mangerud, S.E. Lie, H. Furnes, I.L. Kristiansen and L. Lomo, A Younger Dryas ash bed in western Norway and its possible correlations with tephra in cores from the Norwegian Sea and the north Atlantic, *Quat. Res.* 21, 85–104, 1984.
- [16] T. Kvamme, J. Mangerud, H. Furnes and W. Ruddiman, Geochemistry of Pleistocene ash zones in cores from the North Atlantic, *Nor. Geol. Tidsskr.* 69, 251–272, 1989.
- [17] W.F. Ruddiman and L.K. Glover, Vertical mixing of ice-rafted volcanic ash in North Atlantic sediments, *Geol. Soc. Am. Bull.* 83, 2817–2836, 1972.
- [18] I.L. Kristiansen, J. Mangerud and L. Lomo, Late Weichselian/early Holocene pollen and lithostratigraphy in lakes in the Alesund area, western Norway, *Rev. Palaeobot. Palynol.* 53, 185–231, 1988.
- [19] S. Björck, O. Ingólfsson, H. Hafliðason, M. Hallsdóttir and N.J. Anderson, Lake Torfdalsvatn: a high resolution record of the North Atlantic ash zone 1 and the last glacial–interglacial environmental changes in Iceland, *Boreas* 21, 15–22, 1992.

- [20] W.F. Ruddiman and A. McIntyre, The north Atlantic during the last deglaciation, *Palaeogeogr., Palaeoclimatol., Palaeoecol.* 35, 145–214, 1981.
- [21] L.D. Keigwin and G.A. Jones, Glacial–Holocene stratigraphy, chronology, and paleoceanographic observations on some north Atlantic sediment drifts, *Deep-Sea Res.* 36(6), 845–867, 1989.
- [22] E. Jansen and T. Veum, Evidence for two-step deglaciation and its impact on North Atlantic deep-water circulation, *Nature* 343, 612–616, 1990.
- [23] T.B. Kellogg, J.-C. Duplessy and N.J. Shackleton, Planktonic foraminiferal and oxygen isotopic stratigraphy and paleoclimatology of Norwegian Sea deep-sea cores, *Boreas* 7, 61–73, 1978.
- [24] E. Bard, M. Arnold, J. Duprat, J. Moyes and J.-C. Duplessy, Reconstruction of the last deglaciation: Deconvolved records of $\delta^{18}\text{O}$ profiles, micropaleontological variations and accelerator mass spectrometric ^{14}C dating, *Climate Dyn.* 1, 101–102, 1987a.
- [25] N. Koc and E. Jansen, A high-resolution diatom record of the last deglaciation from the SE Norwegian Sea: documentation of rapid climatic changes, *Paleoceanography* 7(4), 499–520, 1992.
- [26] E. Bard, Correction of accelerator mass spectrometry ^{14}C ages measured in planktonic foraminifera: Paleoceanographic implications, *Paleoceanography* 3, 635–645, 1988.
- [27] J. Jouzel, J.R. Petit, N.I. Barkov, J.M. Barnola, J. Chappellaz, P. Ciais, V.M. Kotlyakov, C. Lorius, V.N. Petrov, D. Raynaud and C. Ritz, The last deglaciation in Antarctica: further evidence of a ‘Younger Dryas’ type climatic event, in: *The Last Deglaciation (NATO ASI 12)*, E. Bard and W.S. Broecker, eds., pp. 229–266, Springer, 1992.
- [28] W.S. Broecker and T.-H. Peng, *Tracers in the Sea*, Eldigio, Columbia University, New York, 1982.
- [29] W.F. Ruddiman, C.D. Sancetta and A. McIntyre, Glacial/interglacial response of the subpolar North Atlantic waters to climatic change: the record in oceanic sediments, *Philos. Trans. R. Soc. London B280*, 119–142, 1977.
- [30] E. Bard, M. Arnold, P. Maurice, J. Duprat, J. Moyes and J.C. Duplessy, Retreat velocity of the North Atlantic polar front during the last deglaciation determined by ^{14}C accelerator mass spectrometry, *Nature* 328, 791–794, 1987b.
- [31] N. Koc, E. Jansen and H. Haflidason, Paleoceanographic reconstructions of surface ocean conditions in the Greenland, Iceland and Norwegian Seas through the last 14 ka based on diatoms, *Quat. Sci. Rev.* 12, 115–140, 1993.
- [32] P. Schlosser, B. Kromer, R. Weppernig, H.H. Loosli, R. Bayer, G. Bonani and M. Suter, The distribution of ^{14}C and ^{39}Ar in the Weddell Sea, *J. Geophys. Res.* 99(C5), 10275–10287, 1994.
- [33] P.A. Mayewski, L.D. Meekler, S. Whitlow, M.S. Twickler, M.C. Morrison, R.B. Alley, P. Bloomfield and K. Taylor, The atmosphere during the Younger Dryas. *Science* 261, 195–197, 1993.
- [34] J.-R. Petit, M. Briat and A. Royer, Ice age aerosol content from east Antarctic ice core samples and past wind strength, *Nature* 293, 391–394, 1981.
- [35] R.S. Keir, Are atmospheric CO_2 content and Pleistocene climate connected by wind speed over a polar Mediterranean Sea? *Global Planet. Change* 8, 59–68, 1993.
- [36] P.S. Liss and L. Merlivat, Air–sea gas exchange rates: Introduction and synthesis, in: *The Role of Air–Sea Exchange in Geochemical Cycling*, P. Buat-Menard, ed., pp. 113–127, Reidel, Hingham, Mass., 1986.
- [37] B. Kromer and B. Becker, German oak and pine ^{14}C calibration, 7200 BC to 9439 BC, *Radiocarbon* 35(1), 125–135, 1993.
- [38] W.S. Broecker, Some thoughts about the radiocarbon budget for the Glacial Atlantic, *Paleoceanography* 4(2), 213–220, 1989.
- [39] S. Manabe and R.J. Stouffer, Two stable equilibria of a coupled ocean–atmosphere model, *J. Climate* 1(9), 841–866, 1988.
- [40] T.F. Stocker and D.G. Wright, Rapid transitions of the ocean’s deep circulation induced by changes in surface water fluxes, *Nature* 351, 729–732, 1991.
- [41] W.S. Broecker, Salinity history of the northern Atlantic during the last deglaciation, *Paleoceanography* 5(4), 459–467, 1990.
- [42] L.D. Labeyrie, J.-C. Duplessy, J. Duprat, A. Juillet-Leclerc, J. Moyes, E. Michel, N. Kallel and N.J. Shackleton, Changes in the vertical structure of the North Atlantic Ocean between glacial and modern times, *Quat. Sci. Rev.* 11, 401–413, 1992.
- [43] S.J. Lehman and L.D. Keigwin, Deep circulation revisited, *Nature* 358, 197–198, 1992b.
- [44] W.J. Schmitz and M.S. McCartney, On the North Atlantic circulation, *Rev. Geophys.* 31(1), 29–49, 1993.
- [45] T. Keffer, D.G. Martinson and B.H. Corliss, On the position of the north Atlantic polar front during Quaternary glaciations, *Science* 241, 440–442, 1988.
- [46] W.S. Broecker, M. Klas, E. Clark, S. Trumbore, G. Bonani, W. Wölfli and S. Ivy, Accelerator mass spectrometry radiocarbon measurements on foraminifera shells from deep sea cores, *Radiocarbon* 32(2), 119–133, 1990b.
- [47] S. Levitus, *Climatological atlas of the world ocean*, NOAA Prof. Pap. 13, 1982.
- [48] W.S. Broecker, T.-H. Peng, G. Ostlund and M. Stuiver, The distribution of bomb radiocarbon in the ocean, *J. Geophys. Res.* 90(C4), 6953–6970, 1985.
- [49] W.S. Broecker and T.-H. Peng, Carbon cycle 1985: Glacial to interglacial changes in the operation of the global carbon cycle, *Radiocarbon* 28(2A), 309–327, 1986.
- [50] U. Siegenthaler, M. Heimann and H. Oeschger, ^{14}C variations caused by changes in the global carbon cycle, *Radiocarbon* 22(2), 177–191, 1980.